Available online at www.sciencedirect.com
ScienceDirect
Journal of Solid State Chemistry 181 (2008) 848–854
JOURNAL OF SOLID STATE CHEMISTRY
www.elsevier.com/locate/jssc

Organically modified porous hydroxyapatites: A comparison between alkylphosphonate grafting and citrate chelation

L. El-Hammari[a], H. Marroun[a], A. Laghzizil[a], A. Saoiabi[a], C. Roux[b], J. Livage[b], T. Coradin[b,c,*]

[a]*Laboratoire de Chimie physique Générale, Faculté des Sciences, B.P. 1014, Rabat, Morocco*
[b]*UPMC Univ Paris 06, UMR 7574, Chimie de la Matière Condensée de Paris, F-75005 Paris, France*
[c]*CNRS, UMR 7574, Chimie de la Matière Condensée de Paris, F-75005 Paris, France*

Received 24 October 2007; received in revised form 11 January 2008; accepted 20 January 2008
Available online 4 February 2008

Abstract

Two alternative methods to prepare organically modified porous hydroxyapatites following a "one pot" approach were compared. The partial substitution of inorganic phosphates by alkylphosphonates leads to mesoporous materials with high specific surface area ($>200\,m^2\,g^{-1}$). The incorporation of the organic moieties within the hydroxyapatite structure is confirmed by Infra-red and solid-state NMR spectroscopy and depends on the nature of the alkyl chain. However, it induces a significant loss of the material crystallinity. In contrast, the introduction of citrate, a calcium-chelating agent, to the precursor solution does not improve the material specific surface area but allows a better control of the hydroxyapatite structure, both in terms of crystallinity and pore size distribution.

Keywords: Hydroxyapatites; Mesoporous materials; Alkylphosphonates; Calcium chelates

1. Introduction

The elaboration of porous hydroxyapatite $Ca_{10}(PO_4)_6(OH)_2$ (HAp) is highly desirable to design biomaterials, adsorbents or catalysts [1–8]. In the case of bone repair materials, a macroporous network with inter-connected cavities is often necessary to ensure osteogenic cells colonization of the HAp implant. In contrast, adsorption of pollutants or toxic ions is favored for materials presenting 2–50 nm pores and a high specific surface area, i.e. mesoporous materials. In addition, the crystallinity and surface chemistry of HAp have a large influence on its adsorption properties [9–12].

Different structure and surface properties of synthetic HAp can be obtained by varying the method and conditions of HAp formation [13–16]. The nature of the calcium (calcium nitrate, hydrated lime, calcium alkoxides) and phosphate (phosphoric acid, ammonium phosphate, phosphorus alkoxide) precursors, the reaction pH and temperature as the presence of an additional solvent are key parameters for the control of the material porosity [14,17]. In parallel the modification of the surface properties of pre-formed HAp materials was widely studied, including pyrophosphoric acid, alkyl phosphates, bisphosphonates [18–21] and long-chain carboxylic acids [22–25].

In contrast to these post-grafting approaches, very few studies have been devoted to the "one pot" grafting of organic functions within HAp materials [26,27]. In such procedures, part of the inorganic phosphate precursor is replaced by an organophosphate molecule. These approaches not only allow the homogeneous grafting of the organic function over the whole material volume but, because the organophosphates can inhibit the growth of calcium phosphate particles, they significantly modify the HAp porous structure. Another possibility to perform simultaneous surface functionalization and structure

*Corresponding author at: UPMC Univ Paris 06, UMR 7574, Chimie de la Matière Condensée de Paris, F-75005 Paris, France.
Fax: +33 144274769.
E-mail address: Thibaud.Coradin@courriel.upmc.fr (T. Coradin).

0022-4596/$ - see front matter © 2008 Published by Elsevier Inc.
doi:10.1016/j.jssc.2008.01.030

control is to use calcium-chelating agents. In this context, several groups studied the influence of citric acid on HAp precipitation demonstrating that the organic ligand controls the calcium phosphate particle size and crystallinity, and is present in the final material [28,29]. However, no detailed information on the HAp porous structure is available so far.

With the aim of comparing these two approaches, we have prepared and characterized organically modified mesoporous HAps formed in the presence of organophosphate grafting agents (methyl- and terbutylphosphonic acids) and by addition of a calcium-chelating ligand (citric acid).

2. Experimental

2.1. Material preparation

The pure HAp was prepared by a modified chemical wet method previously reported [13]: 1.67 mol of $Ca(OH)_2$ and 1 mol of $NH_4H_2PO_4$, corresponding to the HAp stoichiometric ratio of $Ca/P = 1.67$, were independently dissolved in deionized water at room temperature. The phosphorus-containing solution was quickly added to the calcium solution and the mixture stirred for 1 h at 25 °C. The final suspensions were aged for 48 h at room temperature, filtered and thoroughly washed with deionized water. The recovered precipitate was dried overnight at 100 °C in an oven.

Grafted HAp (MPOH/TPOH-HAp) were obtained following a similar procedure except for the phosphorus-containing solutions that were prepared by mixing $(1-x)$ moles of $NH_4H_2PO_4$ with x mol ($x = 0.05$, 0.1 and 0.2) of methylphosphonic acid $CH_3PO(OH)_2$ (MPOH) or terbutylphosphonic acid $(CH_3)_3CPO(OH)_2$ (TPOH).

Citrate-modified HAp (c-HAp) was obtained following a similar procedure as for pure HAp except for the calcium-containing solutions that were prepared by adding 0.25 mol of citric acid to the $Ca(OH)_2$ solution.

2.2. Characterization techniques

The resulting solids were characterized using X-ray powder diffraction (XRD) (Philips PW131 diffractometer, Cu$K\alpha$ radiation). Infra-red spectra were recorded with a 2 cm^{-1} resolution on a Bruker IFS 66v FT-IR spectrophotometer using KBr pellets. Nitrogen sorption isotherms were recorded at 77 K using a Micromeretics ASAP 2010 instrument. The specific surface areas (S_{BET}) and C constant were calculated according to the Brunauer–Emmet–Teller (BET) method, using a value of 16.2 $Å^2$ for the cross-section area of nitrogen. The porous volume (V_p) and pore size (D_p) distribution were estimated using the Barret–Joyner–Halenda (BJH) approximation. When possible, the microporous volume was evaluated using the α-plot method, using a LiChrospher Si-1000 reference. Chemical analyses were performed by AES-ICP (for Ca and P) and by the CNRS micro-analysis center (for C and H).

Grafted HAps were also investigated using ^{31}P and ^{13}C magic angle spinning (MAS) nuclear magnetic resonance (NMR). MAS NMR spectra were recorded on a Bruker Avance 300 (7T) spectrometer operating at 121.5 and 75.7 MHz for ^{31}P and ^{13}C, respectively. ^{31}P spectra were acquired on a 4 mm diameter probe with a MAS rate of 14 kHz. Cross polarization (CP) was used with 3 s of relaxation delay and 2 ms of contact time. ^{13}C spectra were acquired on a 7 mm diameter probe with a MAS rate of 5 kHz. CP was used with 1 s of relaxation delay and 3 ms of contact time. ^{31}P and ^{13}C chemical shift are referenced to H_3PO_4 85% and tetrametylsilane, respectively.

Scanning electron microscopy was performed on gold-coated samples using a Cambridge Stereoscan 120 instrument at an accelerating voltage of 10 kV.

3. Results and discussion

3.1. Phosphonic acid-grafted apatites

X-ray powder diffraction analysis of HAp samples obtained in the presence of MOPH and TPOH after heating at 100 °C overnight are shown in Fig. 1 and compared with the pure HAp sample. For MPOH, all samples exhibit the typical diffraction peaks of the apatite structure including $2\Theta = 26°$ (002), 31° (211) and 33° (300), with a similar poor crystallinity, as indicated by the broad half-peak width (Fig. 1). In contrast, a loss of sample crystallinity with increasing amount of TPOH is observed.

Infra-red spectra of these samples display the vibration mode of PO_4 and OH groups (Fig. 2). The vibrations characteristic of the PO_4 groups are seen at 1090, 1030, 962, 603 and 565 cm^{-1} for pure and organically modified HAp. The fine peaks found at 3560 and 630 cm^{-1} corresponding to the OH group of the crystalline apatite structure that are clearly visible for the HAp powder are

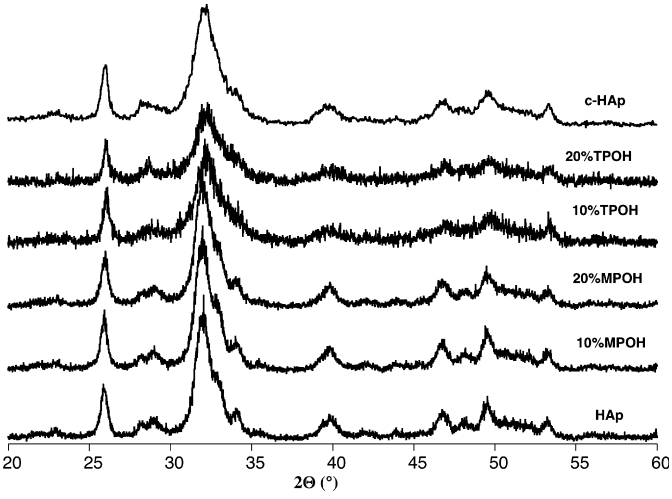

Fig. 1. X-ray diffraction patterns of pure, phosphonic acid-grafted and citrate-modified apatites.

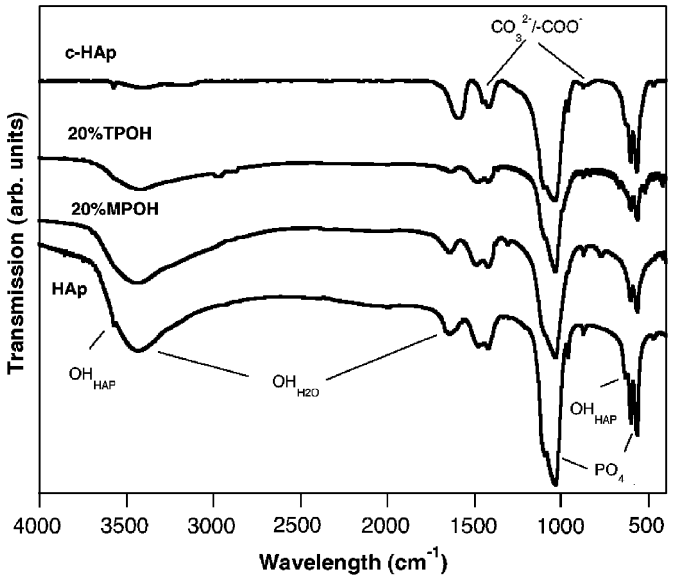

Fig. 2. Infra-red spectra of pure, 20% phosphonic acid-grafted and citrate-modified apatites.

absent from the 20% MPOH/TPOH-HAp samples. In parallel, the broad vibration band at 3500 cm^{-1} and the band at 1610 cm^{-1}, corresponding, respectively, to the OH stretching mode of adsorbed water and the deformation band of water molecule, indicate the high hydration state of recovered powders. Additionally, vibration bands attributed to carboxylates and carbonate groups are observed at 1460, 1430 and 875 cm^{-1}. The presence of the organic groups could be detected by the C–H vibration bands of MPOH, and more significantly TPOH, at 2900–2800 cm^{-1}.

The results of chemical analysis and TGA are gathered on Table 1. The Ca/P ratio are slightly lower than the 1.60 value found for the pure HAp, except for the 20% TPOH-HAp sample, where a Ca/P = 1.54 ratio is found. As expected, the carbon and hydrogen content are seen to increase with the amount of incorporated alkylphosphonate species. This result is confirmed by TGA analysis (not shown) where the weight loss in the 350–700 °C temperature domain, corresponding to organic matter degradation, is also observed to increase with MPOH and TPOH initial content. However, whereas the initial ratio of carbon atoms for MPOH over TPOH is 4, the carbon contents found for 20% MPOH and 20% TPOH lead to a carbon ratio <3 within the HAp material, indicating a more limited incorporation of the terbutylphosphonate when compared to the methylphosphonate. A more careful examination of the material composition was performed after calculation of C/Ca and C/P molar ratio (Table 1). Neglecting carbonates and atmospheric carbon pollution, it is found that the TPOH/P molar ratio is similar in the initial solution and final material whereas the MPOH/P ratio in the material is twice as high as in the precursor solution. This suggests that, in the latter case, the phosphonic acid incorporation occurred at the detriment

Table 1
Chemical composition of pure, phosphonic acid-grafted and citrate-modified apatites

Samples	Ca/P	% C	% H	C/Ca	CP	Δm (%)
HAp	1.60	0.13	1.25	0.01	0.02	<1
10% MPOH	1.60	1.27	1.74	0.11	0.19	1.5
20% MPOH	1.58	2.17	2.02	0.21	0.34	2.0
10% TPOH	1.59	2.93	2.07	0.26	0.41	3.5
20% TPOH	1.54	5.86	2.25	0.60	0.89	5.5
c-HAp	1.61	4.7	–	0.44	0.70	7.0

The calcium-to-phosphorus ratios (Ca/P) were obtained from ICP-AES data, the carbon (%C) and hydrogen (%H) contents from microanalysis and the weight loss in the 350–700 °C temperature domain (Δm) from TGA. Carbon-to-calcium (C/Ca) and carbon-to-phosphorus (C/P) molar ratios were obtained from calculation.

of inorganic phosphates. Although this hypothesis requires further analysis to be confirmed, it appears in good agreement with literature data indicating specific interactions between Ca^{2+} and MPOH [32].

The presence of organics within the apatite structure is also checked by ^{13}C MAS NMR (Fig. 3(b)). All samples contain carbonate groups (156 ppm), in agreement with IR data. The 10% MPOH-HAp material shows an additional resonance at 13 ppm corresponding to the C atom of the CH_3 group of methylphosphonic acid. In the presence of TPOH, resonances are observed between 25 and 30 ppm corresponding to the carbon atoms of the terbutyl group. In order to get more information on the nature of organophosphate environment within the apatite structure, the samples were investigated using ^{31}P MAS NMR. The ^{31}P MAS NMR spectra of pure HAp and 10% MPOH/TPOH-HAp materials are shown in Fig. 3(a). The pure apatite sample shows a unique peak at 2.5 ppm, in good agreement with previous data [13,30,31]. In the presence of MPOH, two additional bands are found at ca. 25 and 31 ppm whereas a weak broad signal in the 25–45 ppm range observed for TPOH. As MPOH and TPOH both show a unique resonance at ca. 25 ppm in solution [33], these data indicate that part of the organophosphates is weakly adsorbed on the apatite surface. The appearance of additional signals down-field shifted by ca. 6–10 ppm suggest the existence of stronger interactions. However, it is worth noticing that the post-grafting of phosphonic acid on HAp surface usually leads to an up-field shift of the ^{31}P signal [34]. However, the here-observed reverse effect was previously reported for MPOH in solution in the presence of Ca^{2+} [32], suggesting that the "one pot" approach developed here allows a more intimate mixing of the organophosphonates with the apatite precursors. It is worth noting that these NMR data alone do not allow to fully ascertain the incorporation of phosphonic acid in the apatite structure, this assumption is supported by the fact that no other phase are observed on the XRD pattern. In addition, SEM images of the different materials indicate that they have a homogenous structure (Fig. 4), another

argument against a possible precipitation of a phase-separated phosphonic acid calcium salt.

The porous structure of the materials was investigated by nitrogen sorption. Corresponding isotherms are shown on Fig. 5. All materials exhibit similar type IV isotherms typical of mesoporous materials. However, it worth noting that for all grafted materials, the $(P/P_0)_h$ relative pressure, corresponding to the onset of the hysteresis, is shifted to lower values when compared to the pure HAp sample. Remarkably, a shift from $(P/P_0)_h = 0.65$ for HAp to $(P/P_0)_h = 0.45$ is observed for 10% TPOH and remain unmodified for 20% TPOH whereas a progressive decrease in $(P/P_0)_h$ is observed in the presence of MPOH from a 0.60 value for 10% MPOH to 0.45 for 20% MPOH. These observations suggest that incorporation of organophosphates can efficiently modulate the average size of the mesopores. This is confirmed by the calculated S_{BET}, V_p and average D_p gathered in Table 2. All grafted samples have a similar specific surface area S_{BET} of ca. 240–250 $m^2 g^{-1}$, significantly higher than the pure HAp sample ($S_{BET} = 140\ m^2 g^{-1}$). In the presence of TPOH, the porous volume progressively increases from $V_p = 0.42\ cm^3 g^{-1}$ for HAp to $0.51\ cm^3 g^{-1}$ for 10% TPOH-HAp and $0.59\ cm^3 g^{-1}$ for 20% TPOH-HAp. The calculated pore size distribution (Fig. 6) indicates that the pure HAp exhibit a pore population distributed around a maximum diameter value of ca. 80 Å whereas, in the presence of 10% TPOH, a narrow population centered at ca. 35 Å appears together with a broad population of larger pores. This results in a significant decrease of the average pore size, from $D_p = 120$ Å for HAp to $D_p = 80$ Å for 10% TPOH-HAp. With 20% TPOH, a similar distribution profile is observed but the broad population is now shifted to larger pore size, resulting in an increase of the average pore size to ca. 100 Å. For 10% MPOH, the porous volume is significantly higher than for the pure HAp ($V_p = 0.73\ cm^3 g^{-1}$) but the pore size distribution and average pore size $D_p = 110$ Å are very similar to the reference sample. In contrast, as already suggested by isotherm profiles, the 20% MPOH sample porous structure is very similar to the TPOH-containing samples, in terms of pore size distribution, average pore size $D_p = 90$ Å and porous volume $V_p = 0.55\ cm^3 g^{-1}$.

Calculation of the C constant of the BET equation indicates a significant decrease of the surface adsorption energy from the pure HAp to the organically modified apatites and a limited decrease with grafting amount and number of carbons of the phosphonic acid molecule (Table 2). This is in good agreement with the increased hydrophobicity of these surfaces with organic modification. In addition, analysis of the microporosity of the samples

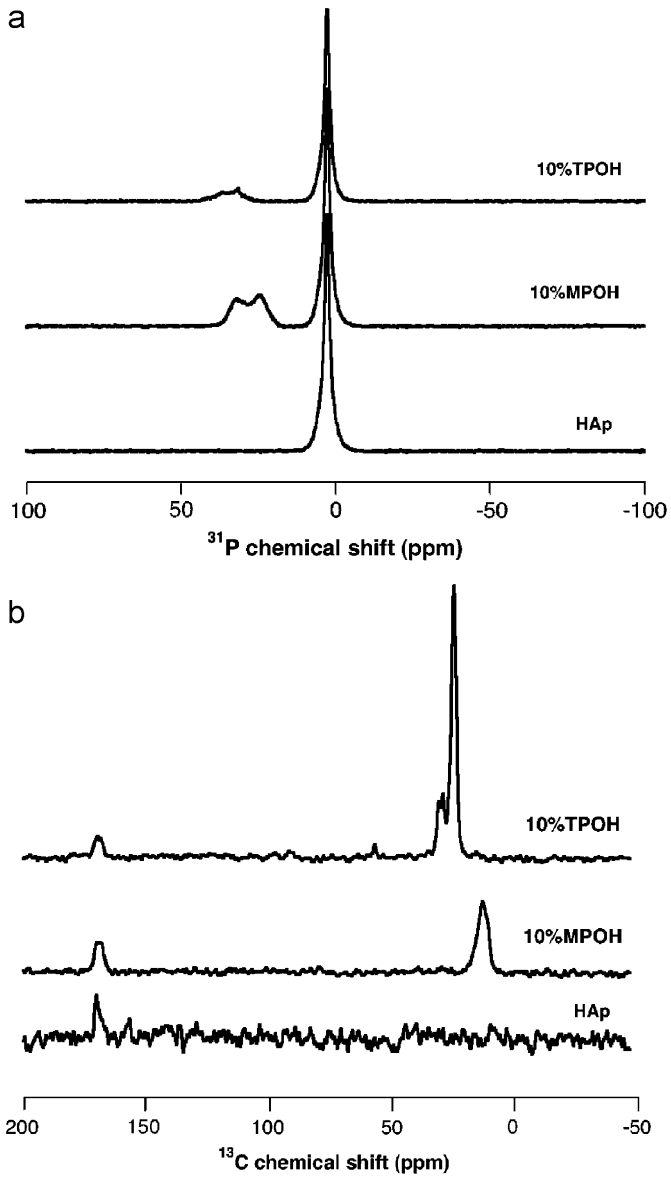

Fig. 3. ^{31}P MAS NMR (a) and ^{13}C MAS NMR (b) spectra of pure and 10% phosphonic acid-grafted apatites.

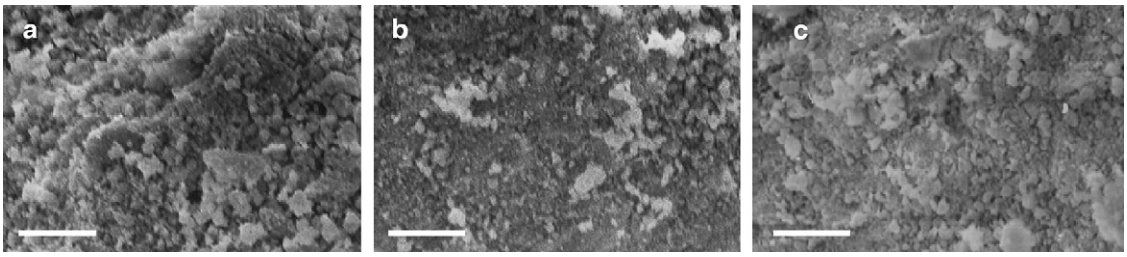

Fig. 4. SEM micrographs of (a) pure, (b) 10% MPOH-grafted and (c) 10% TPOH-grafted apatites (scale bar = 10 μm).

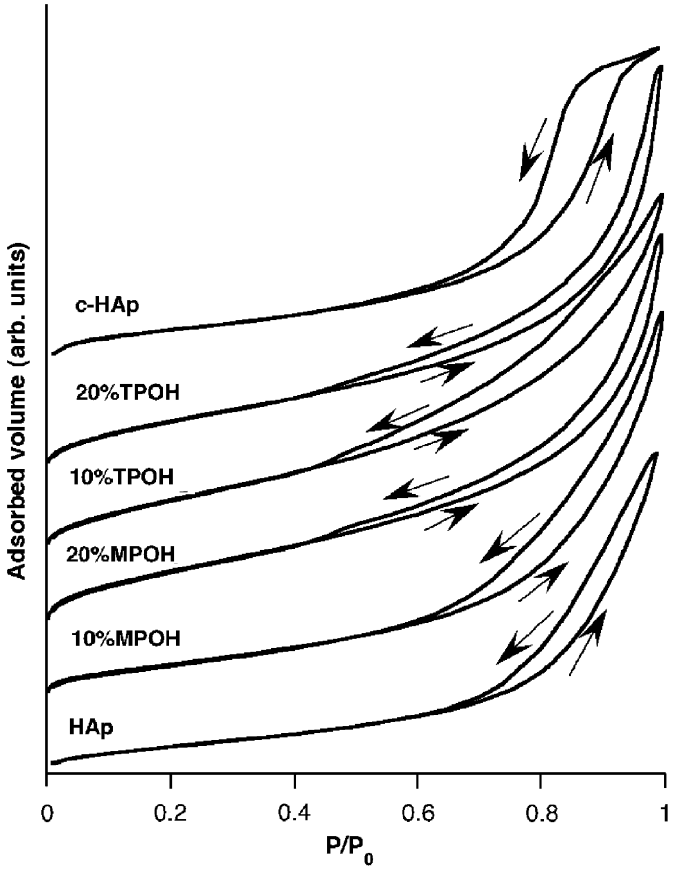

Fig. 5. N_2-sorption isotherms of pure, phosphonic acid-grafted and citrate-modified apatites. Upwards and downwards arrows are for adsorption and desorption data, respectively.

Table 2
Porous characteristics of pure, phosphonic acid-grafted and citrate-modified apatites

Samples	S_{BET} ($m^2 g^{-1}$)	V_p ($cm^3 g^{-1}$)	D_p (Å)	C	$(P/P_0)_h$
HAp	140	0.42	120	130	0.65
10% MPOH	255	0.73	110	45	0.60
20% MPOH	255	0.55	90	40	0.45
10% TPOH	240	0.51	80	30	0.45
20% TPOH	240	0.59	100	25	0.45
c-HAp	155	0.18	60	80	0.65

Specific surface area (S_{BET}), porous volume (V_p), average pore size (D_p),C constant and relative pressure at the onset of hysteresis ($(P/P_0)_h$) were calculated from the N_2-sorption isotherms.

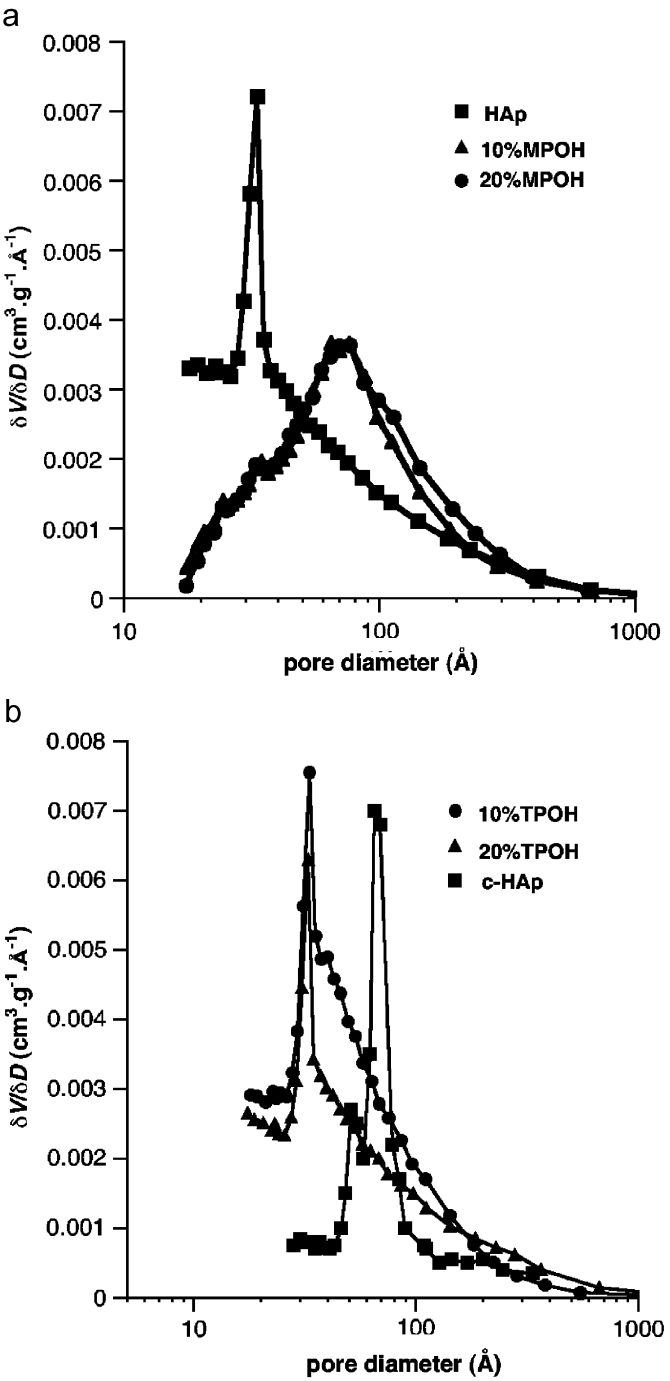

Fig. 6. Pore size distribution ($\delta V/\delta D$) of (a) pure and MPOH-grafted apatites and (b) TPOH-grafted and citrate-modified apatites.

was performed using the α-plot approach using a hydrophilic macroporous silica reference. A limited microporous volume ($\approx 0.01\,cm^3 g^{-1}$) was found for HAp whereas a more significant value was calculated for 10% MPOH ($\approx 0.11\,cm^3 g^{-1}$). In the latter case, the BET method leads to an over-estimation of the specific surface area that was recalculated to be ca. $205\,m^2 g^{-1}$. For the other samples, the obtained α-values could not be interpreted, due to the hydrophobic nature of the surfaces, but the shape of the isotherms also suggests the presence of a significant microporosity.

3.2. Comparison with citrate-modified apatites

The XRD diffractogram of c-HAp is very similar to one of the pure HAp, suggesting that the presence of citrate has a limited impact on the apatite crystallinity (Fig. 1). The IR spectra confirm the presence of phosphate and carbonate

groups, as well as adsorbed water (Fig. 2). As far as apatite hydroxyl groups are concerned, the band located at 3560 cm^{-1} is clearly visible, in contrast with previous phosphonic acid-grafted materials. Moreover, two bands are found in the 3000–3500 cm^{-1} region and a change in the intensity of the bands at 1400 and 1600 cm^{-1} is observed, corresponding, respectively, to the OH and C=O vibration mode of carboxyl groups, as already observed for apatite grown in the presence of citrate [35,36].

This is confirmed by chemical analysis and TGA data (Table 1) that indicate a 4.7% carbon content in the c-HAp sample and a ca. 7% organic matter content. In the same time, the Ca/P ratio is the same as for HAp, suggesting that the presence of citrate did not inhibit the growth of the apatite structure or favor the formation of other calcium phosphate phases. In addition, ^{31}P MAS NMR spectrum of c-HAp is found similar to the spectra of pure HAp (not shown), suggesting no significant perturbation of the apatite structure by the citrate ligand.

The nitrogen sorption isotherm of c-HAp is shown in Fig. 5 and exhibits again a typical type IV shape. No significant shift in the $(P/P_0)_h$ relative pressure value is observed. However, in the high P/P_0 pressure domain, the c-HAp isotherm is characterized by a well-defined plateau indicating a closed mesoporosity whereas the reference sample does not exhibit such a plateau, suggesting the presence of an open mesoporosity. In parallel, the c-HAp S_{BET} specific surface area is very close to the one of HAp but this material possesses a much lower porous volume (Table 2). In the same time, the pore size distribution of c-HAp is narrow and centered around ca. 60 Å (Fig. 6).

It therefore appears that the presence of citrate influences the apatite formation in a very different way than organophosphates. In the first case, the ligand was suggested to interact with the formed calcium phosphate nuclei during the growth phase, resulting in smaller apatite particles. As a result, inter-particle aggregation leads to smaller pores when compared to pure HAp, as observed here. However, the c-HAp material exhibits the same specific surface area but smaller porous volume than the un-modified HAp, meaning that fewer pores are accessible, which may result from porosity filling by citrate molecules. The fact that Ca/P ratio is not modified by citrate addition also supports the hypothesis that the ligand does not interfere with the nucleation of the HAp phase but only with the growth process. In contrast, organophosphates appear to have a much profound influence on HAp formation. Several evidences, including the loss of crystallinity, the decrease of the Ca/P ratio and of the intensity of IR vibration band of the HAp OH group with increasing MPOH and TPOH and the ^{31}P NMR data, suggest that these organic molecules may play a role on both the nucleation and growth of the calcium phosphate phase, i.e. on the chemical composition and crystallite size. In parallel, the aggregation of such disorganized particles leads to the modification of the pore size distribution. Interestingly, the resulting porous structure appears as a mixture of the HAp network exhibiting widely distributed large pores and c-HAp structure consisting of narrowly distributed smaller pores. One explanation would be that two populations of apatite particles are present, with the smallest ones formed under organophosphate control and the largest ones consisting of pure HAp crystallites. This hypothesis is supported by the comparison of pore size distribution in 10% TPOH-HAp and 20% TPOH-HAp where the increase in phosphonic acid content is correlated with an increase of the smallest pore population to the detriment of much larger ones.

Finally, it is worth noting that TPOH appears more efficient than MPOH in influencing the HAp formation, although its rate of incorporation within the mineral structure is lower. It suggests that the steric hindrance introduced by the alkyl chain of the phosphonic acid has a two-side effect as it may limit the incorporation of the organic phosphate within the apatite structure while its adsorption on the calcium phosphate nuclei surface may more efficiently inhibit further particle growth.

4. Conclusions

Two approaches were evaluated to obtain organically modified mesoporous HAps. The addition of alkylphosphonates is efficient in increasing the apatite porosity by influencing the calcium phosphate nucleation and growth. However, this enhancement of the material porosity occurs at the detriment of its crystallinity, as already observed for phenylphosphate additives. In contrast, the introduction of a calcium-chelating agent, citrate, leads to an apatite structure with a low specific area but with a well-defined porous structure and minor loss of crystallinity. Further investigations are now in progress to evaluate the effect of other carboxylic acids with the hope of increasing the material porous volume, in order to design more efficient HAp-based adsorbents.

Acknowledgment

The authors thank G. Laurent (CMCP) for his help in NMR experiments.

References

[1] J.C. Elliott, Structure and Chemistry of the Apatites and other Calcium Orthophosphates, Elsevier, Amsterdam, 1994.
[2] K.S. Vecchio, X. Zhang, J.B. Massie, M. Wang, C.W. Kim, Acta Biomater. 3 (2007) 910–918.
[3] L. Pang, Y. Hu, Y. Yan, L. Liu, Z. Xiong, Y. Wei, J. Bai, Surf. Coatings Technol. 24 (2007) 9549–9557.
[4] L. El Hammari, A. Laghzizil, A. Saoiabi, P. Barboux, S. Brandès, R. Guilard, Adsorp. Sci. Technol. 24 (2006) 507–516.
[5] X. Shen, H. Tong, T. Jiang, Z. Zhu, P. Wan, J. Hu, Compos. Sci. Technol. 24 (2007) 2238–2245.
[6] S.K. Dehury, V.S. Hariharakrishnan, Tetrahedron Lett. 4 (2007) 2493–2496.

[7] N. Yoshida, M. Takeuchi, T. Okura, H. Monma, M. Wakamura, H. Ohsaki, T. Watanabe, Thin Solid Films 50 (2006) 108–111.
[8] R. Atir, S. Mallouk, K. Bougrin, A. Laghzizil, M. Soufiaoui, Synth. Commun. 36 (2006) 11.
[9] K. Kandori, S. Tsuyama, H. Tanaka, T. Ishikawa, Colloids Surf. B 58 (2007) 98–104.
[10] P.K. Ng, J. He, P. Gagnon, J. Chromatogr. A 1141 (2007) 13–18.
[11] B. Sandrine, N. Ange, B.A. Didier, Ch. Eric, S. Patrick, J. Hazard. Mater. 139 (2007) 443–446.
[12] G. del Río, P. Sanchez, P.J. Morando, D.S. Cicerone, Chemosphere 64 (2006) 1015–1020.
[13] L. El Hammari, A. Laghzizil, A. Saoiabi, P. Barboux, M. Meyer, Colloids Surf. A 289 (2006) 84–88.
[14] L. El Hammari, H. Merroun, T. Coradin, S. Cassaignon, A. Laghzizil, A. Saoiabi, Mater. Chem. Phys. 104 (2007) 448–453.
[15] K. Kanazawa, Inorganic Phosphate Materials, Studies in Inorganic Chemistry, vol. 18, Elsevier, Amsterdam, London, New York, Tokyo, 1989.
[16] Y.X. Pang, X. Bao, J. Eur. Ceram. Soc. 23 (2003) 1697–1704.
[17] K. Cheng, G. Shen, W. Weng, G. Han, J.M.F. Ferreira, J. Yang, Mater. Lett. 51 (2001) 37–41.
[18] H. Denissen, E. van Beek, C. Lowik, S. Papapoulos, A. van der Hooff, Bone Miner. 25 (1994) 123–134.
[19] M. Yoshinari, Y. Oda, T. Inoue, K. Matsuzaka, M. Shimono, Biomaterials 23 (2002) 2879–2885.
[20] H. Roussiere, G. Montavon, S. Laib, P. Janvier, B. Alonso, F. Fayon, M. Petit, D. Massiot, J.-M. Bouler, B. Bujoli, J. Mater. Chem. 15 (2005) 3869–3875.
[21] G. Nancollas, R. Tang, R. Phipps, Z. Henneman, S. Gulde, W. Wu, A. Mangood, R. Russell, F. Ebetino, Bone 38 (2006) 617–627.
[22] H. Tanaka, M. Futaoka, R. Hino, J. Colloid Interf. Sci. 269 (2004) 358–363.
[23] H. Tanaka, A. Yasukawa, K. Kandori, T. Ishikawa, Colloids Surf. A 125 (1997) 53–62.
[24] O.G. da Silva, E.C. da Silva Filho, M.G. da Fonseca, L.N.H. Arakaki, C. Airoldi, J. Colloid Interf. Sci. 302 (2006) 485–491.
[25] H.W. Choi, H.J. Lee, K.J. Kim, H.M. Kim, S.C. Lee, J. Colloid Interf. Sci. 304 (2006) 277–281.
[26] A. Wang, H. Yin, D. Liu, H. Wu, M. Ren, T. Jiang, X. Cheng, Y. Xu, Mater. Lett. 61 (2007) 2084–2088.
[27] A. Aissa, M. Debbabi, M. Gruselle, R. Thouvenot, P. Gredin, R. Traksmaa, K. Tõnsuaadu, J. Solid State Chem. 180 (2007) 2273–2278.
[28] A. Lopez-Macipe, J. Gomez-Morales, R. Rodriguez-Clemente, J. Colloid Interf. Sci. 200 (1998) 114–119.
[29] J.A.M. van der Houwen, E. Valsami-Jones, Environ. Technol. 22 (2001) 1325–1329.
[30] L. El Hammari, A. Laghzizil, P. Barboux, A. Saoiabi, K. Lahlil, J. Solid State Chem. 177 (2004) 134–138.
[31] L.M. Rodriguez-Lorenzo, J. Mater. Sci.: Mater. Med. 16 (2005) 393–398.
[32] M. DeFronzo, R.J. Gillies, J. Biol. Chem. 262 (1987) 11032–11037.
[33] I. Lukes, M. Borbaruah, L.D. Duin, J. Am. Chem. Soc. 116 (1994) 1737–1741.
[34] D. Fukegawa, S. Hayakawa, Y. Yoshida, K. Suzuki, A. Osaka, B. van Meerbeek, J. Dent. Res. 85 (2006) 941–944.
[35] J.A.M. van der Houwen, G. Cressey, B.A. Cressey, E. Valsami-Jones, J. Cryst. Growth 249 (2003) 572–583.
[36] L.J. Brecevic, H. Füredi-Milhofer, Calcif. Tissue Int. 28 (1979) 131–136.